

A toolbox to find the best mechanistic model to predict the behavior of environmental systems

van Turnhout, André G.; Kleerebezem, Robbert; Heimovaara, Timo J.

DOI

[10.1016/j.envsoft.2016.05.002](https://doi.org/10.1016/j.envsoft.2016.05.002)

Publication date

2016

Document Version

Accepted author manuscript

Published in

Environmental Modelling & Software

Citation (APA)

van Turnhout, A. G., Kleerebezem, R., & Heimovaara, T. J. (2016). A toolbox to find the best mechanistic model to predict the behavior of environmental systems. *Environmental Modelling & Software*, 83, 344-355. <https://doi.org/10.1016/j.envsoft.2016.05.002>

Important note

To cite this publication, please use the final published version (if applicable). Please check the document version above.

Copyright

Other than for strictly personal use, it is not permitted to download, forward or distribute the text or part of it, without the consent of the author(s) and/or copyright holder(s), unless the work is under an open content license such as Creative Commons.

Takedown policy

Please contact us and provide details if you believe this document breaches copyrights. We will remove access to the work immediately and investigate your claim.

Manuscript Number: ENVSOFT-D-15-00385R3

Title: A toolbox to find the best mechanistic model to predict the behavior of environmental systems.

Article Type: Research Paper

Keywords: Bayesian inference; mechanistic biogeochemical modeling; integrative assessment of environmental systems; qualitative and quantitative model selection; optimal data description

Corresponding Author: Mr. André Gerard van Turnhout, Ir.

Corresponding Author's Institution: TU Delft

First Author: André Gerard van Turnhout, Ir.

Order of Authors: André Gerard van Turnhout, Ir.; Robbert Kleerebezem, Dr. Ir.; Timo J Heimovaara, Dr. Ir.

Abstract: Reliable prediction of the long-term behavior of environmental systems such as Municipal Solid Waste (MSW) landfills is challenging. While many driving forces influence this behavior, characterization of them is limited by measurement techniques. Therefore, a model structure for reliable prediction needs to optimally combine all measured information with suitable mechanistic information from literature. How to get such an optimal model structure? This study presents a toolbox to find and build the model structure that describes an environmental system as close as possible. The toolbox combines environmental frameworks to include all suitable mechanistic information; it fully couples kinetic and equilibrium reactions and contains multiple resources to obtain biogeochemical parameters.

Several possible optimal model structures are quickly built and evaluated with objective statistical performance criteria obtained via Bayesian inference. By applying the novel methodology, we select the best model structure for anaerobic digestion of MSW in full scale landfills.

Response to Reviewers: There were no comments from the reviewers.

Dear editor,

Thank you for your fast reply, we are very happy that our manuscript is considered for publication in *Environmental Modelling & Software* (EM&S). We also thank you for your additional comments which enabled us to improve the transparency and framing of the presented methodology and results. We double checked the grammar in the paper and changed the following according to your comments.

In line 55, we included two citations of papers from EM&S (Vrugt et al. (2016) and Kelly et al. (2013)) which express the need for a more objective integrated assessment of environmental systems. These are included to show that novel methods such as the one we present are necessary to decrease uncertainty in modeling of environmental systems. Our toolbox decreases model uncertainty by combining mechanistic information from different environmental fields and evaluating models based on qualitative and quantitative criteria.

In line 56, we included a reference to Bennett et al. (2013) who propose a generic evaluation procedure of model performance. Such an approach strengthens the credibility and relevance of modelling reported which is in line with the methodology we present. In lines 83-92, we indicate that our method supports all five evaluation steps proposed by Bennett et al. (2013). In our evaluation, however, the step of checking the data is minimal because the available measured data and information about its error was very limited. Nevertheless, we believe that the characteristics of our novel methodology are sufficiently demonstrated and that the best model is satisfactory given the scope of the paper.

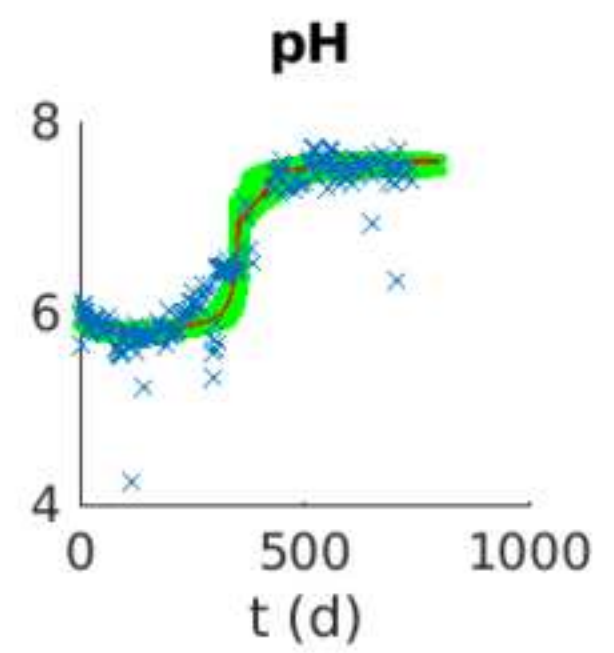
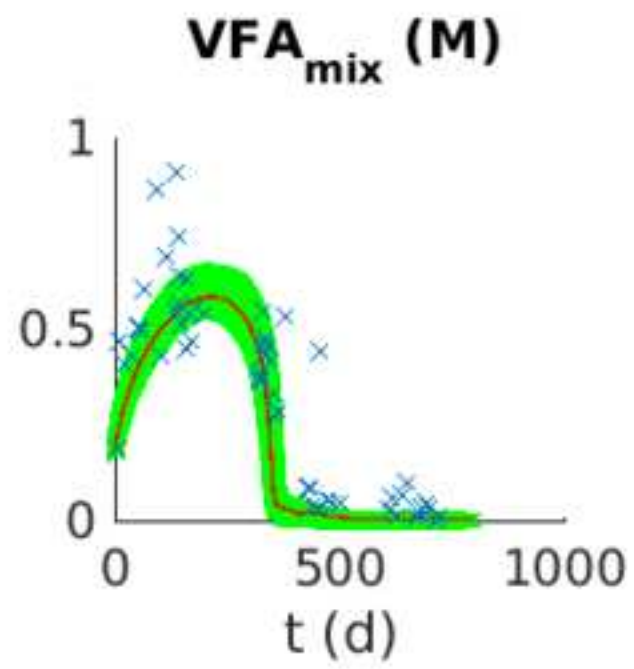
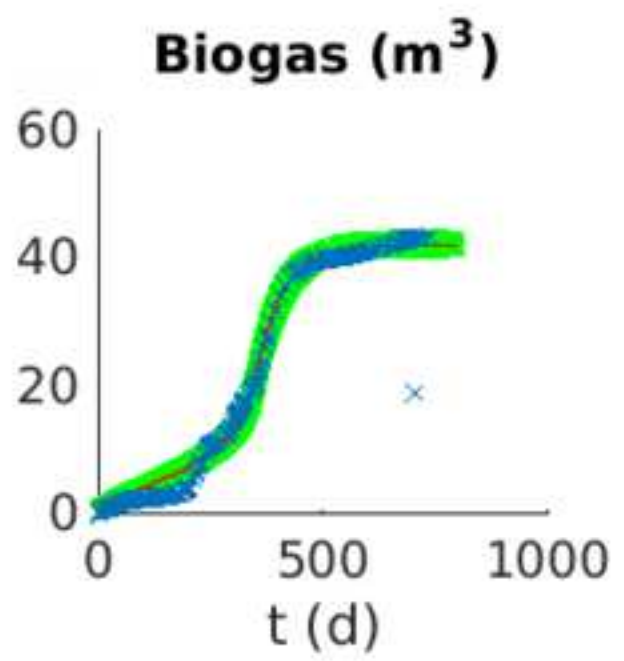
In section 2.4, we added a subsection describing the qualitative performance criteria that are generated by the toolbox. In section 2.4.3, we justify our choice in quantitative criteria. We chose a set of criteria that enabled us to quantify aspects related to the (mechanistic) uncertainty of the models which is in line with the purpose of our modeling exercise. In addition, we indicate that other criteria suited for other modeling purposes are readily implemented.

Results and discussion are only slightly modified because we believe that the changes made in the introduction and theory already improved their framing and justification significantly. Furthermore, we modified the conclusion about the best model into two steps. First we conclude which model is best for lysimeter scale and then we conclude which model is best for full scale.

We thank you for your time and hope our paper is now fit to contribute to *Environmental Modelling & Software*.

Sincerely yours,

André van Turnhout



Highlights

- Finding the best mechanistic model to predict the behavior of environmental systems.
- The toolbox allows to quickly assess multiple biogeochemical reaction networks.
- Coupled kinetic & equilibrium processes and mechanistic parameter resources.
- Networks are evaluated with objective statistical criteria given measured data.
- The toolbox enabled to find the optimal network for anaerobic digestion of MSW.

A toolbox to find the best mechanistic model to predict the behavior of environmental systems.

Illustrated by modeling anaerobic degradation of Municipal Solid Waste

André G. van Turnhout^{a,*}, Robbert Kleerebezem^b, Timo J. Heimoaara^a

^a*Geoscience & Engineering Department, Faculty of CiTG, Delft University of Technology, Stevinweg 1, 2628CN, Delft, Netherlands*

^b*Environmental Technology Group, Department of Biotechnology, Delft University of Technology, Julianalaan 67, 2628 BC, Delft, Netherlands*

Abstract

Reliable prediction of the long-term behavior of environmental systems such as Municipal Solid Waste (MSW) landfills is challenging. While many driving forces influence this behavior, characterization of them is limited by measurement techniques. Therefore, a model structure for reliable prediction needs to optimally combine all measured information with suitable mechanistic information from literature. How to get such an optimal model structure? This study presents a toolbox to find and build the model structure that describes an environmental system as close as possible. The toolbox combines environmental frameworks to include all suitable mechanistic information; it fully couples kinetic and equilibrium reactions and contains multiple resources to obtain biogeochemical parameters. Several possible optimal model structures are quickly built and evaluated with objective statistical performance criteria obtained via Bayesian inference. By applying the novel methodology, we select the best model structure for anaerobic digestion of MSW in full scale landfills.

Keywords: Bayesian inference, mechanistic biogeochemical modeling, integrative assessment of environmental systems, qualitative and quantitative model selection, optimal data description

1. Introduction

It is challenging to make reliable predictions of the long-term behavior of environmental systems such as Municipal Solid Waste (MSW) landfills. In such systems, there are many driving forces influencing behavior, while current measurement techniques are not sufficient to characterize them. Therefore, for reliable predictions we require a mechanistic description with minimal uncertainty for extrapolation of measured data.

Reliable prediction of long-term emissions is needed for landfill management. Decisions about ending of landfill after care strongly depend on these predictions because after care can only be stopped

*Corresponding author, email address: a.g.vanturnhout@tudelft.nl
Preprint submitted to Elsevier

1
2
3
4
5 when emissions are below certain threshold values. Furthermore, reliable predictions also improve
6 estimations of energy recovery from emissions such as methane. This energy is directly utilized in the
7 facilities at the landfill.
8
9

10 So far, prediction of emissions by any modeling strategy is highly uncertain. In general, models
11
12 have been developed according to two strategies. One strategy extrapolates measured emissions using
35 empirical relations. Some of these models fit exponential equations to measured gas and leachate
13 data [6, 32, 9, 13]. Others apply neural networks on emission data [26, 14]. Although the fit of
14 these empirical models with measured data is very good, their extrapolations are poor because these
15 models are not constrained by mechanistic principles. These models do not consider the impact of
16
17 changes in environmental conditions on the emissions while multiple studies have shown that e.g. pH
18 and mass transport limitation significantly influence the performance of waste water and solid waste
19
40 treatment[34, 3, 1, 40, 42].
21
22
23

24 The other modeling strategy to predict emissions is mechanistic [29, 45, 20, 8, 7, 17]. These
25 models vary a lot in complexity and the type of mechanistic information they include. Model concepts
26
27 range from single point to three dimensional implementation and from a single type of framework
45 such as biochemistry to frameworks coupling biochemistry, hydrology and settlement. Although these
28 models do restrict their predictions with mechanistic principles and have given interesting insights,
29 their prediction accuracy is often also very poor. Prediction with these models is poor because the
30 uncertainty in mechanistic assumptions is very large, especially for very complex models. In addition it
31
32 is difficult to reduce this uncertainty by model calibration because measured data is limited. The large
33
50 uncertainty in mechanistic correctness is reflected by the wide spread of parameter values published
34 in literature [22].
35
36
37
38
39

40 To improve prediction accuracy, the challenge is to select a model structure that is constrained by
41 mechanistic principles and has minimum uncertainty in assumptions. In order to find such a model,
42
43 a more objective integrated assessment of environmental systems is needed [43, 15] in which model
55 performance evaluation is generalized [4]. This type of assessment requires several prerequisites for
44 developing models. First, mechanisms from different environmental fields should be available to be
45 combined in order to include all suitable mechanistic information. Second, well established mechanistic
46 parameters with relative low uncertainty should be readily obtainable from databases or derivation
47
48 methods. Third, model performance should be able to be analyzed qualitatively and quantitatively.
49
50 Statistical analysis of the remaining uncertainty in parameters in light of the measured data should
51
60 allow us to quantify the uncertainty in model structure, calibrated parameter values and mechanistic
52 correctness of the model. Finally, multiple reaction networks should be able to be quickly built and
53
54
55
56
57
58
59
60
61
62
63
64
65

1
2
3
4
5 the results quickly assessed in order to find the optimal model. Current modeling approaches do not
6
7 fulfill all these prerequisites and therefore limit the possibility to find optimal models for prediction
8
9 purposes.

10 The aim of this study is to develop a methodology that includes all the prerequisites previously
11 mentioned in order to enable us to find an optimal mechanistic model for anaerobic degradation of
12 MSW. The toolbox allows us to quickly build mechanistic biogeochemical reaction networks that may
13
14 include kinetic reactions, equilibrium reactions and environmental inhibitions in a multi-phase system.
15
16 Parameter values are obtained from an extensive geochemical database [21], a derivation method
17 based on thermodynamic principles [16] and calibration based on measured data. Performances of
18 these reaction networks are evaluated quantitatively with statistical criteria obtained by applying
19 Bayesian inference with the DREAM algorithm [44, 18]. We illustrate our generic approach by finding
20
21 an optimal mechanistic model for describing a data set measured on a series of landfill lysimeters,
22
23 previously published by Valencia et al. [36, 37, 35, 38, 39], by evaluating four possible reaction
24
25 networks. Our aim is to find a description which we can apply to full-scale anaerobic landfills.
26
27

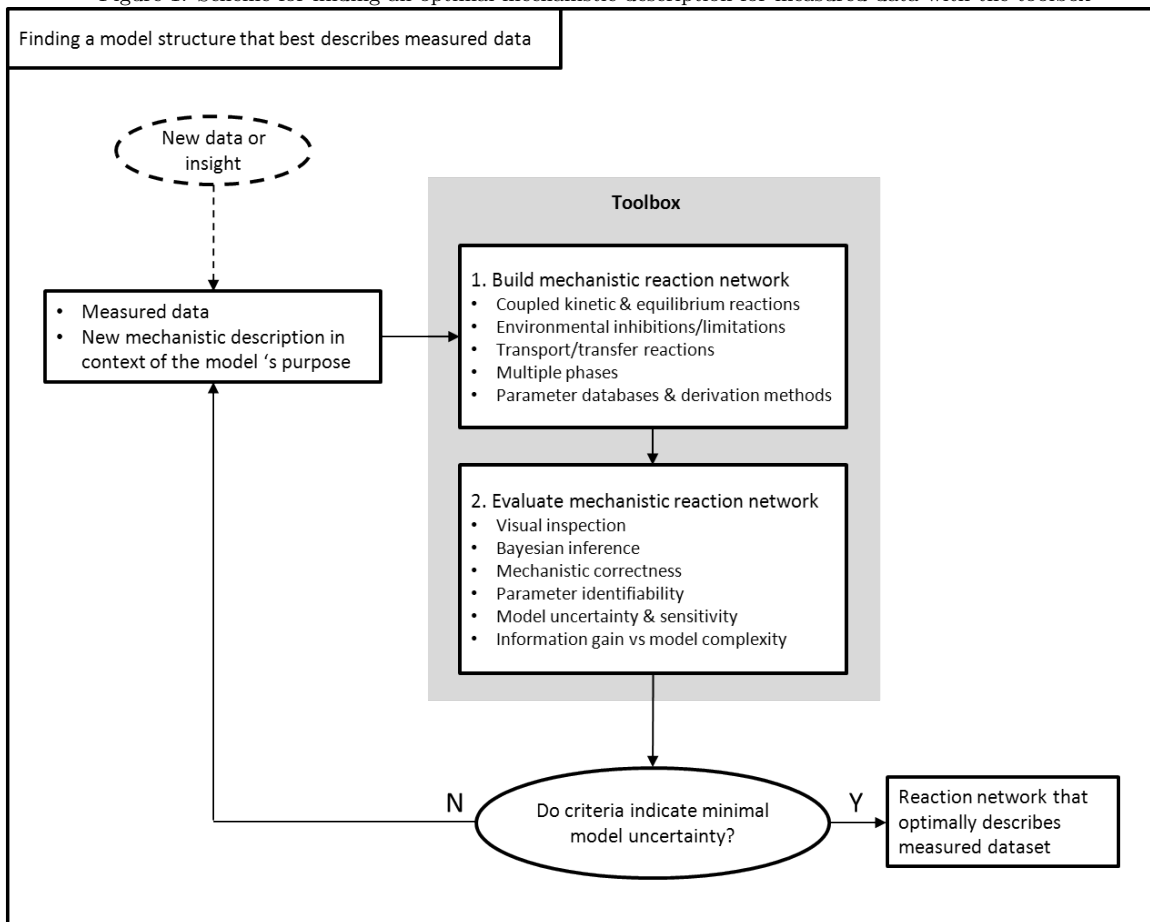
28 **2. Theory**

29 *2.1. The cycle of finding an optimal model structure*

30
31
32 The toolbox we present here is a novel combination of several approaches enabling us to find an
33
34 optimal mechanistic model for describing measured data. This method follows the scheme depicted
35
36 in figure 1 and allows a generic evaluation of model performance such as proposed by Bennett et al.
37 (2013) [4]. We start by defining a first possible mechanistic reaction network which should provide a
38
39 good fit to the measured data.

40
41 Subsequently, this reaction network is evaluated qualitatively by plotting the modeled data against
42
43 the measured data and quantitatively by using a range of performance criteria which we obtain by
44
45 applying Bayesian inference on the most uncertain parameters. These criteria allow us to judge aspects
46
47 such as mechanistic correctness, parameter identifiability, model uncertainty, model sensitivity and
48
49 model complexity. Based on the results and the purpose of the model, we decide if the model describes
50
51 the measured data with sufficient (mechanistic) accuracy. If the accuracy is not sufficient, a next
52
53 iteration is started where an update to the reaction network is evaluated until an optimal model is
54
55 found. All prerequisites combined in the toolbox are discussed in detail below.
56
57
58
59
60
61
62
63
64
65

Figure 1: Scheme for finding an optimal mechanistic description for measured data with the toolbox



2.2. Defining the model structure with mechanistic information from different environmental frameworks

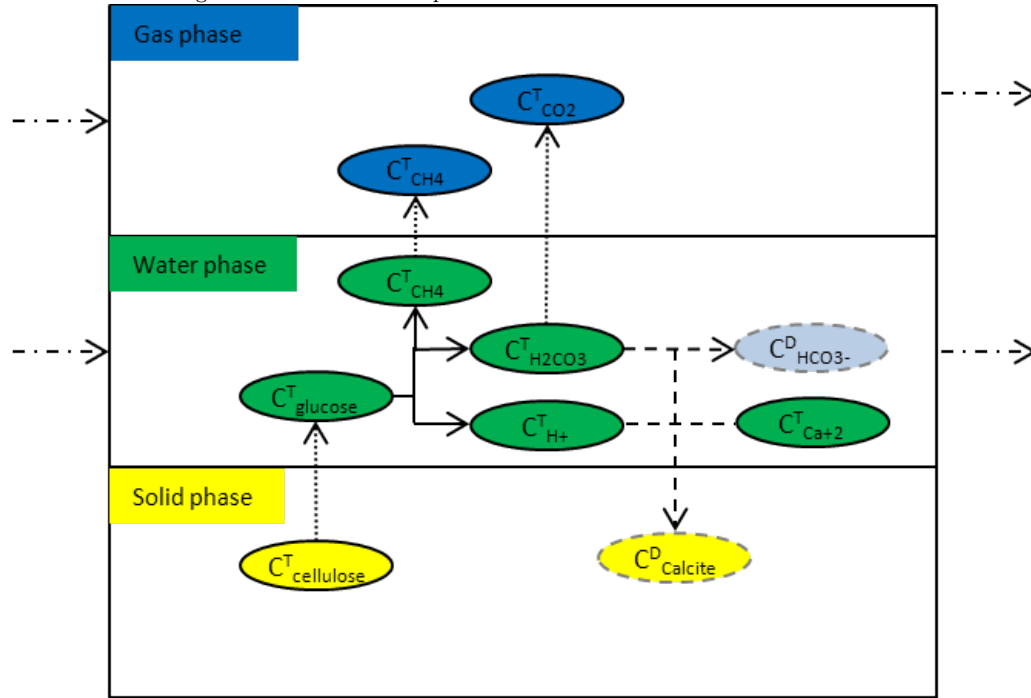
2.2.1. Multiphase, multicomponent and multiprocess environment

Model structures can be built that contain biogeochemical reaction networks within a multiphase environment with mass transport across the model domain and mass transfer between the phases. A schematic example of such a structure is given in figure 2. The model describes the fate of chemical compounds present in the solid, gas and liquid phase. In each phase we track the change of the total concentrations (C_{ref}^T) and derived concentrations (C^D) as a function of time. Total concentrations are calculated with the mass balances of building blocks of species e.g. H^+ and CO_3^{-2} which are expressed in terms of one reference species. Using chemical equilibrium approaches, we can calculate the derived concentrations from the set of total concentrations (i.e. mass balances). Changes in total concentrations with time are caused by kinetic processes which can be either biochemical redox reactions, transfer of compounds between phases and transport in or out of the model domain. Biochemical

reactions are influenced by environmental inhibitions and limitations.

To support quick implementation of a model structure, it is completely defined within a single spreadsheet and solved with a generic matrix calculation method.

Figure 2: Schematic example of a model structure that can be build with the toolbox



C_i^T	Total concentration i (of all species together)→	Mass transfer between phases
C_i^D	Derived concentration i (of one species)	→	Kinetic reaction acting on total concentrations
- - ->	Mass transport in/out of the phase	- - ->	Equilibrium reaction acting on a species

2.2.2. Fully coupled rate dependent and equilibrium processes

Rate dependent processes and equilibrium processes are fully coupled within the model structure. This means that all derived concentrations are automatically recalculated when the total concentrations change because of biochemistry and transport or transfer processes. For example, the total concentration of H₂CO₃ in a standard water-carbonate system (i.e. $C_{H_2CO_3}^T$, $C_{Ca^{+2}}^T$ and $C_{H^+}^T$) changes because of gas production. The model updates the $C_{H_2CO_3}^T$ and as a result the pH and concentrations of CO₃⁻², HCO₃⁻, H₂CO₃ and CaCO₃ are automatically updated. Full coupling allows accurate calculation of derived concentrations and their influence on the rate dependent processes in the system.

1
2
3
4
5
6
7
8
9
10
11
12
13
14
15
16
17
18
19
20
21
22
23
24
25
26
27
28
29
30
31
32
33
34
35
36
37
38
39
40
41
42
43
44
45
46
47
48
49
50
51
52
53
54
55
56
57
58
59
60
61
62
63
64
65

Details on how to derive concentrations from mass balances according to equilibrium reactions are given in Bethke et al. (2008) [5].

2.2.3. Type of rate dependent processes

120 Biogeochemical reaction rates ($R_{C_i^T}^K$) are implemented as

$$R_{C_i^T}^K = \mu^{\max} \cdot C^{T'} \cdot I \cdot s_i \quad (1)$$

125 where μ^{\max} is the maximum rate, $C^{T'}$ is the concentration that drives the reaction, I is the total inhibition factor ranging from 0 to 1 and s_i is the stoichiometry. This type of reaction supports Monod kinetics when the inhibition factor is (partly) determined by substrate limitation and the total concentration of bacteria is set as the driving concentration.

The rates of change in the liquid phase (p_l) and the gas phase (p_g) due to the presence of a mass transfer flux between phases are implemented as

$$F_{C_i^{T,p_l}}^{\text{MF}} = k_1 a \cdot \left(C_i^{p_l'} - C_i^{p_g'} \cdot K_H \cdot R \cdot T \right) \quad (2)$$

$$F_{C_i^{T,p_g}}^{\text{MF}} = F_{C_i^{T,p_l}}^{\text{MF}} \cdot \frac{V_l}{V_g} \quad (3)$$

130 where $k_1 a$ is the mass transfer constant, $C^{p_l'}$ and $C^{p_g'}$ are the driving concentrations (total or derived) in the water phase and the gas phase, K_H is the Henry coefficient, T is the temperature, R is the universal gas constant, V_l is the volume of the water phase and V_g is the volume of the gas phase.

The rate of change due to a mass transport flux ($F_{C_i^T}^{\text{MT}}$) is implemented as

$$F_{C_i^T}^{\text{MT}} = \frac{\phi \cdot C_i^T}{V} \quad (4)$$

135 where ϕ is the mass transport flow and V is the volume of the phase.

2.2.4. Type of equilibrium processes

Two types of equilibrium processes can be implemented in a model structure. The first type is a true equilibrium reaction relating concentrations of species according to mass action law. The second type is an equilibrium between the gas and the liquid phase. This equilibrium is implemented using mass transfer reactions (eq. 2) with high values for $k_1 a$.

2.2.5. Environmental inhibitions and limitations

Rate inhibiting and limiting reaction terms are implemented using four mechanisms of biochemical reactions taken from environmental studies (equations 5 to 8). These are substrate limitation (f^{SL}) [23], non-competitive inhibition (f^{NC}) [10], inhibition of sulphate reduction by sulfide (f^{SS}) and inhibition

1
2
3
4
5
6
7
8
9
10
11
12
13
14
15
16
17
18
19
20
21
22
23
24
25
26
27
28
29
30
31
32
33
34
35
36
37
38
39
40
41
42
43
44
45
46
47
48
49
50
51
52
53
54
55
56
57
58
59
60
61
62
63
64
65

145 of sulphate reduction by protonated Volatile Fatty Acids (VFA) (f^{SA}) [31]. In these equations, C_{inh} is the inhibiting concentration (either a total or derived concentration), K_{inh} is the inhibition or half saturation constant and l is a shape parameter. Each mechanism gives an inhibition factor f ranging from 0 to 1. Multiplication of all inhibition factors acting on a biochemical reaction gives its total inhibition factor I (eq. 1).

$$150 \quad f_{(C_{\text{inh}})}^{\text{SL}} = \frac{C_{\text{inh}}}{C_{\text{inh}} + K_{\text{inh}}} \quad (5)$$

$$17 \quad f_{(C_{\text{inh}})}^{\text{NC}} = \left(\frac{K_{\text{inh}}}{K_{\text{inh}} + C_{\text{inh}}} \right)^l \quad (6)$$

$$20 \quad f_{(C_{\text{inh}})}^{\text{SS}} = \left(1 - \frac{C_{\text{inh}}}{K_{\text{inh}}} \right)^l \quad (7)$$

$$24 \quad f_{(C_{\text{inh}})}^{\text{SA}} = \left(1 + \left(\frac{C_{\text{inh}}}{K_{\text{inh}}} \right)^l \right)^{-1} \quad (8)$$

2.2.6. Selecting mechanistic parameter values from databases and derivation methods

155 Parameter values or bandwidths are entered into the spreadsheet where the model structure is defined. The geochemical parameters for the equilibrium reactions are automatically retrieved from an extensive geochemical database which is part of the Orchestra chemical equilibrium model ([21]). A wide variety in validated geochemical equilibria can be selected. As an option, activity correction can be calculated with the Davies equation.

160 Stoichiometry and rate parameters of biochemical metabolic reactions can be derived from thermodynamic principles with an additional spreadsheet. This derivation method is adapted from Kleerebezem and van Loosdrecht, (2010) [16]. It allows to constrain the model with established mechanistic information.

As an example, we illustrate the method with the derivation of a metabolic reaction for methanogenesis. Metabolism is a combination of catabolism (releasing energy) and anabolism (biological growth) which are coupled using the yield factor,

$$165 \quad Y_{\text{xs}} = \frac{\text{CmolX}}{\text{CmolS}} \quad (9)$$

which specifies how much growth (X) occurs from substrate (S) given the amount of energy generated by the catabolic reaction. CmolX is the number of moles of C in the biomass and CmolS is the number of moles of C in the substrate. The redox half reactions for catabolism can be written as



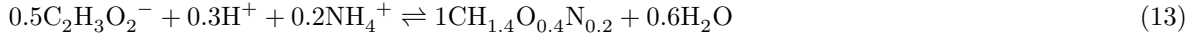


10
11
12
13
14
15
16
17
18
19

which combine to the following catabolic reaction:

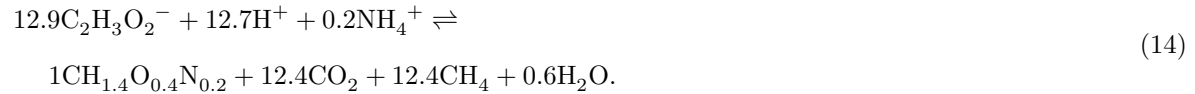


175 Following the same principle, the anabolic reaction is as follows,



17 where we assume the generic molecular composition of bacteria ($\text{CH}_{1.4}\text{O}_{0.4}\text{N}_{0.2}$) to be the same as used by Henze et al. (1995) [12].

20 The growth yield is calculated with the method proposed by Kleerebezem and van Loosdrecht,
21 (2011). This is a partially empirical method based on the Gibbs reaction energy of the catabolic and
180 22 anabolic reaction [11]. In this case, $Y_{\text{xs}} = 0.04$ which leads to the following total metabolic reaction:



23 In addition to the stoichiometry, also the rate parameters for metabolic reactions can be estimated
24 from thermodynamic principles [11].

25
26
27
28
29
30
31
32
33
34
35
36
37
38
39
40

185 Estimated parameter values can be corrected for temperature using several relations. Maximum rates, equilibrium constants and the solubility of Calcite are corrected with equations 15-17 respectively [41] [28]. In these equations, T_e is the temperature of the environment, T_r is the reference temperature of the parameter, ΔH^0 is the standard enthalpy, k is $64 \frac{\text{kJ}}{\text{mol}}$, a is -171.9065, b is 0.077993, c is 2893.319 and d is 71.595.

41
42
43

$$190 \ln(\mu_e^{\text{max}}) = \ln(\mu_r^{\text{max}}) + \ln\left(\frac{k}{R} \cdot \left(\frac{1}{T_r} - \frac{1}{T_e}\right)\right) \quad (15)$$

$$44 \ln(K_e) = \ln(K_r) + \ln\left(\frac{\Delta H^0}{R \cdot T_r^2} \cdot (T_e - T_r)\right) \quad (16)$$

$$46 \log_{10}(K_{\text{eq}(\text{Calcite})}) = a + b \cdot T_e + \frac{c}{T_e} + d \cdot \log_{10}(T_e) \quad (17)$$

47
48
49
50

2.3. Solving the model structure with a generic matrix calculation method

51 The model structure is automatically assembled in to a system of ordinary differential equations
52 (ODE) with a generic matrix calculation method adapted from Reichel et al. (2007) [29]. This system
195 53 of ODEs is fully coupled with the equilibrium calculator ORCHESTRA [21]. The ODEs are solved in
54 MATLAB and the equilibrium calculator is part of the JAVA memory space of MATLAB. This makes
55
56
57
58
59
60
61
62
63
64
65

the algorithm very efficient since both solvers use the same memory space while information about the total and derived concentrations are exchanged via a JAVA link.

200 The set of ODEs for each phase can be written as

$$\frac{d\mathbf{C}^{\text{T},\text{water}}}{dt} - \mathbf{F}^{\text{T},\text{water}} = \mathbf{R}^{\text{K}} \quad (18)$$

$$\frac{d\mathbf{C}^{\text{T},\text{gas}}}{dt} - \mathbf{F}^{\text{T},\text{gas}} = 0 \quad (19)$$

where \mathbf{F}^{T} are the total fluxes into the respective phase and \mathbf{R}^{K} are the total biochemical rates. The total concentrations in the solid phase are included in the ODEs of the water phase and are expressed per volume of water phase. The total fluxes $\mathbf{F}^{\text{T},\text{water}}$, $\mathbf{F}^{\text{T},\text{gas}}$ and the total biochemical rates \mathbf{R}^{K} are calculated by vector summation over the number of fluxes or reactions j per process,

$$\mathbf{R}^{\text{K}} = \boldsymbol{\mu}^{\text{max}} \circ \mathbf{C}^{\text{T}'} \circ \mathbf{I} \cdot \mathbf{S} \quad (20)$$

$$\mathbf{F}^{\text{T},\text{water}} = \sum_j \mathbf{F}^{\text{MT},\text{water}} - \sum_j \mathbf{F}^{\text{MF},\text{water}} \quad (21)$$

$$\mathbf{F}^{\text{T},\text{gas}} = \sum_j \mathbf{F}^{\text{MF},\text{gas}} - \sum_j \mathbf{F}^{\text{MT},\text{gas}} - \mathbf{x} \cdot \sum \left(\sum_j \mathbf{F}^{\text{MF},\text{gas}} - \sum_j \mathbf{F}^{\text{MT},\text{gas}} \right) \quad (22)$$

210 where $\boldsymbol{\mu}^{\text{max}}$, $\mathbf{C}^{\text{T}'}$ and \mathbf{I} have size $1 \times j$, \circ is the symbol for element-wise multiplication, \mathbf{S} are the stoichiometry with size $j \times n_1$, $\mathbf{F}^{\text{MF},\text{water}}$ and $\mathbf{F}^{\text{MT},\text{water}}$ have size $j \times n_1$, $\mathbf{F}^{\text{MF},\text{gas}}$ and $\mathbf{F}^{\text{MT},\text{gas}}$ have size $j \times n_g$ and \mathbf{x} are the molar fraction of the total concentrations in the gas phase. The last term in $\mathbf{F}^{\text{T},\text{gas}}$ constrains the gas phase with a constant volume and a constant total pressure.

2.4. Evaluating model performance

215 2.4.1. Qualitative evaluation

Model performance is evaluated visually by automatically generated plots combining the model results with the measured data and plots of all modeled states. Because of the strong human capacity for pattern detection, these plots may indicate extreme, under- or non-modeled behavior. In addition, residuals are evaluated with QQ plots and auto-correlation plots.

220 2.4.2. Applying Bayesian inference

In order to find a model structure which provides the best fit to the data, we also evaluate the outcome of the simulation with several objective criteria. All these criteria are evaluated using the results of Bayesian inference applied to the set of most uncertain parameters ($\boldsymbol{\theta}$). The outcome of Bayesian inference,

$$225 \quad p(\boldsymbol{\theta}|\hat{\mathbf{y}}) \propto p(\boldsymbol{\theta}) \cdot L(\boldsymbol{\theta}|\hat{\mathbf{y}}), \quad (23)$$

1
2
3
4
5 is the joint posterior probability distribution ($p(\boldsymbol{\theta}|\hat{\mathbf{y}})$) of the set of parameters given the measured
6 data. This distribution reflects the uncertainty in the different parameters. The posterior distribution
7 is calculated from the prior distribution of the parameters ($p(\boldsymbol{\theta})$) and the likelihood of the parameters
8 in light of the measured data ($L(\boldsymbol{\theta}|\hat{\mathbf{y}})$). The posterior distribution is obtained using an adapted
9 version of the DREAM_(ZS) algorithm [44, 18] where algorithmic settings and parameters are set to the
10 recommended and default values.

11
12
13
14
15 The toolbox uses a Gaussian objective function, which includes the set of standard deviations of
16 total error ($\boldsymbol{\sigma}$) for each subset of data, to evaluate the likelihood,

$$17 \ln(L(\boldsymbol{\theta}|\hat{\mathbf{y}})) = -\frac{n}{2} \cdot \ln(2\pi) - \sum \ln(\boldsymbol{\sigma}) - \frac{1}{2} \cdot \sum \left(\frac{\hat{\mathbf{y}} - \mathbf{y}}{\boldsymbol{\sigma}} \right)^2 \quad (24)$$

18
19
20
21
22
23
24
25
26
27
28
29
30
31
32
33
34
35
36
37
38
39
40
41
42
43
44
45
46
47
48
49
50
51
52
53
54
55
56
57
58
59
60
61
62
63
64
65

235 where \mathbf{y} is the modeled data and $\boldsymbol{\sigma} = [\boldsymbol{\sigma}_{(m \times 1)}^{\text{subset1}}; \boldsymbol{\sigma}_{(m \times 1)}^{\text{subset2}}; \dots]$ with m being the size of a subset of data
and all entries in $\boldsymbol{\sigma}_{(m \times 1)}$ have the same value σ^{subset} for that subset. Because it is often difficult to
estimate the measurement error, and it is more or less impossible to estimate the model error, we chose
to expand the set of uncertain parameters $\boldsymbol{\theta}$ with the standard deviations σ^{subset} for each dataset.

Prior distributions of uncertain model parameters are assumed to be uniform with an initial search
range that is 100× wider to ensure global convergence. Prior distributions of standard deviations are
also uniform ranging from $\frac{1}{5} \cdot \sigma^{\text{subset}}$ to $5 \cdot \sigma^{\text{subset}}$. Ranges in the prior distributions can be different
for other problems.

2.4.3. Quantitative criteria

The result from the Bayesian inference allows us to quantitatively compare the performance of
different model structures. Since our modeling objective is to find the model structure with minimal
(mechanistic) uncertainty, we implemented criteria that quantify aspects related to this. For other
modeling objectives, other criteria/metrics [4, 43] may be more suited which are readily implemented.

One criterion is the difference in best fit or lowest total error (measurement error & model error)
between model structures. In addition, we can also assess the probability distribution of total errors
which is related to the combined probability distributions in calibrated parameters. The latter directly
reflects the uncertainty of the complete model structure in light of the measured data. Even more,
the uncertainty of total error per subset of data can be compared between models with the marginal
probability distributions of the standard deviations.

A second criterion is the uncertainty in calibrated parameters for different model structures. Param-
eter uncertainty is quantified by the width of its marginal posterior distribution. A wider distribution
indicates more uncertainty under the condition of the same prior distribution. For a quantitative

comparison, the gain of information from marginal prior to marginal posterior for parameter i can be quantified with the Kullback-Leibler divergence (D_{KL}). This metric,

$$D_{\text{KL}} = \int (p(\theta_i|\hat{\mathbf{y}}) \cdot \ln \left(\frac{p(\theta_i|\hat{\mathbf{y}})}{p(\theta_i)} \right) \cdot d\theta_i, \quad (25)$$

is a non-symmetric measure of the dissimilarity between two probability distributions. Higher values of D_{KL} indicate a larger information gain and therefore less uncertainty.

A third criterion is the presence of correlations between parameters in the model structure which can be seen in the marginal posterior distributions. These correlations point to possibilities for optimizing model structure by adding restrictions or lumping of correlated parameters.

A fourth criterion is the mechanistic completeness of model structure. Mechanistic completeness is evaluated by comparing the calibrated parameter bandwidths (i.e. 5%-95% quantiles) with 'ideal' parameter values measured under non-limiting conditions. A close match between calibrated parameters and 'ideal' values indicates a mechanistically complete model structure. Parameters that strongly deviate from 'ideal' values indicate missing mechanistic processes.

A final criterion is the amount of information a model structure provides given its complexity. More complex models with a large number of parameters can be compared with simpler ones with the marginalized likelihood (L^{m}) which is the probability of the measured data given the model structure, not assuming any particular model parameters. It can be approximated with the harmonic mean of likelihoods [24],

$$L^{\text{m}} = \left(\frac{1}{N} \sum_{i=1}^N L(\boldsymbol{\theta}|\hat{\mathbf{y}})^{-1} \right)^{-1} \quad (26)$$

where N is the number of likelihoods. The model structure with the highest marginal likelihood has the best balance between information content and model complexity.

3. Results

3.1. The final four evaluated biogeochemical reaction networks

The dataset we used for testing our toolbox was obtained from Roberto Valencia [39, 36]. We present the final four model structures that were the outcome of our search for an optimal model with the methodology provided by the toolbox. These four reaction networks are schematically depicted in Figure 3. In this figure, the most simple network 1 is presented with black lines. Our hypothesis for this network is that four kinetic reactions control the measured emissions. The first one is hydrolysis lumped with acidogenesis. It converts the available biodegradable Solid Organic Matter (SOM) into a mix of Volatile Fatty Acids (VFA_{mix}) with hydrolysis as rate limiting step. The second one is

1
2
3
4
5 methanogenesis which converts the VFA_{mix} into methane and carbon dioxide. The final two reactions
6 are decay of the two types of bacteria involved in lumped hydrolysis and methanogenesis with rates
7 which are 5% of the maximum growth rates [1]. Furthermore, only methanogenesis is influenced by
8
9 substrate limitation of VFA_{mix} . The stoichiometry of the kinetic reactions is listed in table 1. We
10
11 included the most common geochemical equilibrium reactions assuming a readily available excess of
12 Calcite to represent the high alkalinity of MSW. In addition, we assume that the exchange between
13 concentrations in the gas and liquid phases is instantaneous.
14

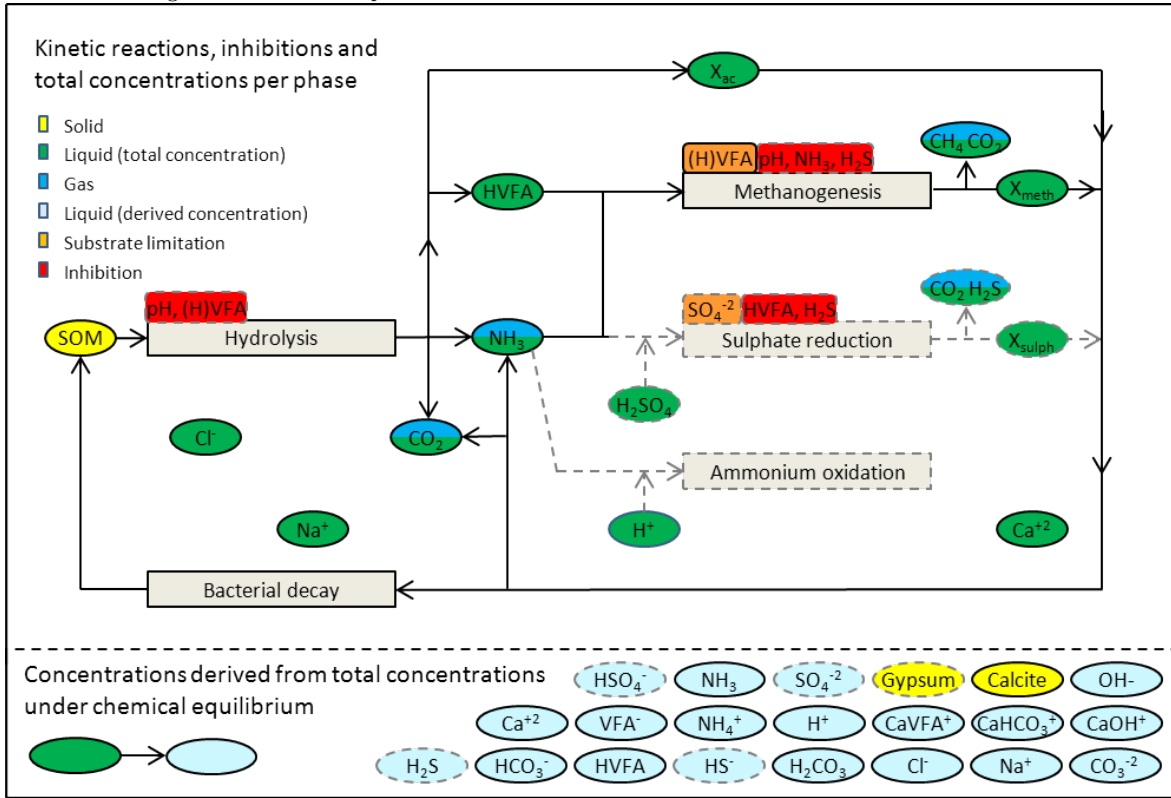
15
16 According to the experimental design, gas vents to the atmosphere and no other transport flows
17
18 are included. Because leachate was recirculated during the experiment, we simplified the problem to
19
20 ideally mixed batch conditions. Model parameters which we considered to be well known are taken
21 from literature. These parameter values are listed in table 2 together with the initial experimental
22 conditions. The model parameters which we considered to be unknown or uncertain are listed in table
23 3 together with the prior ranges found in literature. These unknown parameters in the model's reaction
24
25 network are obtained via Bayesian inference which fits the model outputs to the measurements.
26
27

28 For reaction network 2, we increased the complexity by adding the main environmental inhibitions
29 that are known to influence the kinetic reactions in wastewater treatment. These inhibitions are non-
30 competitive inhibition of hydrolysis by pH and total concentration of VFA_{mix} and non-competitive
31 inhibition of methanogenesis by pH and ammonia.
32

33
34 In reaction network 3, we further increased the complexity by adding a kinetic ammonium oxidation
35
36 reaction. We implemented this reaction to find an explanation for the decreasing measured ammonium
37 concentration in time which normally does not occur under anaerobic conditions.
38

39 Finally, network 4 extends the reaction network further in order to include sulphate and sulfide.
40 These compounds are usually present in anaerobic environments and are known to inhibit methanogen-
41
42 esis and oxidize available biodegradable SOM. Adding mechanistic information about these processes
43 may therefore optimize model performance. The following is included: 1) a kinetic sulphate reduc-
44
45 tion reaction, 2) corresponding equilibrium reactions, 3) inhibition of methanogenesis by H_2S and 4)
46 inhibition of sulphate reduction by H_2S and protonated VFA_{mix} .
47
48
49
50
51
52
53
54
55
56
57
58
59
60
61
62
63
64
65

Figure 3: Schematic representation of the final four reaction networks that were evaluated.



The most basic reaction network 1 is presented with the black lines. Complexity is increased stepwise from network 1-4 which is indicated by the dashed gray lines. Network 2 includes inhibition of hydrolysis by pH and $\text{C}_{\text{VFA}_{\text{mix}}}^{\text{T}}$ and inhibition of methanogenesis by pH and ammonia. In network 3, an ammonium oxidation reaction is added. Network 4 is extended with sulphate reduction for which total concentrations, derived concentrations and inhibitions are included accordingly. X represents bacterial biomass. Compounds that are in equilibrium between the gas phase and the liquid phase have two colors.

1
2
3
4
5
6
7
8
9
10
11
12
13
14
15
16
17
18
19
20
21
22
23
24
25
26
27
28
29
30
31
32
33
34
35
36
37
38
39
40
41
42
43
44
45
46
47
48
49

Table 1: Stoichiometry for the total concentrations in the biochemical reactions

	SOM ³⁾	VFA _{mix} ³⁾	H ₂ CO ₃	NH ₃	H ₂ O	CH ₄	SO ₄ ⁻²	H ₂ S	X _{acid}	X _{meth}	X _{sulph}	H ⁺
Hydrolysis ¹⁾	-1	0.3	0.01	0.024	-0.088	-	-	-	0.18	-	-	-
Methanogenesis	-	-6.67	7.23	-0.2	-8.76	9.37	-	-	-	1	-	-
Decay ²⁾	0.92	-	0.08	0.14	-0.42	-	-	-	(-1)	(-1)	(-1)	-
Ammonium oxidation	-	-	-	-1	-	-	-	-	-	-	-	-1
Sulphate reduction	-	-10.6	27.1	-0.2	-27.1	-	-15.3	15.3	-	-	1	-30.5

The gray cells highlight the reaction driving concentrations. 1) In this reaction, the growth yield for acidogenesis on glucose is used: $Y_{XS} = 1.09$. 2) Each bacterial biomass (X) decays individually. 3) The elemental compositions of SOM is $CH_{1.79}O_{0.63}N_{0.06}$ and VFA_{mix} is $C_{2.64}H_{5.28}O_2$ which were derived from the data measured in the lysimeter experiments.

Table 2: Model parameters and initial conditions

			K_{inh}	l	Initial conditions					
μ_{aci}^{max}	0.12	[1]	$f_{(hyd, C_{H^+}^D)}^{NC}$	1×10^{-5}	2	[34]	$C_{SOM}^{T^1}$	5.44	$C_{Cl^-}^T$	0.1
μ_{decay}^{max}	$0.05 \cdot \mu_{growth}^{max}$	[1]	$f_{(hyd, C_{VFA}^T)}^{NC}$	2.34×10^{-2}	1	[34]	$C_{SO_4^{-2}}^T$	0.16	V_g	250
K_{H,CH_4}	1.5×10^{-3}	[2]	$f_{(meth, C_{H^+}^D)}^{NC}$	5×10^{-7}	2	[34]	$C_{NH_3}^T$	0.065	p_{tot}	1
K_{H,NH_3}	71.4	[2]	$f_{(meth, C_{NH_3}^D)}^{NC}$	1.5×10^{-3}	1	[34]	$C_{H_2CO_3}^T$	1.13	T	303
K_{H,H_2S}	0.11	[2]	$f_{(meth, C_{H_2S}^D)}^{NC}$	4.29×10^{-2}	1	[27]	$C_{Ca^{+2}}^T$	1.16	pH	6.15
K_{H,H_2O}	2.3×10^3	[2]	$f_{(sulph, C_{H_2S}^D)}^{SS}$	1.61×10^{-2}	0.401	[31]	$C_{Na^+}^T$	0.2	V_1	325
K_{H,CO_2}	0.03	[2]	$f_{(sulph, C_{HVFA}^D)}^{SA}$	9×10^{-4}	1.08	[31]				

1) Initial concentration of SOM is taken from the total amount of carbon produced as biogas in the experiment. Units of maximum rates, Henry constants, inhibition constants, concentrations, temperatures, pressures and volumes are respectively d^{-1} , $\frac{mol}{L \cdot atm}$, $\frac{mol}{L}$, $\frac{mol}{L}$, atm, K and L. All parameter values are corrected for 303K except $K_{inh, C_{H_2S}^D}$ (298 K).

3.2. Outcome of the Bayesian inference applied on the four networks

The result of the Bayesian inference allows us to evaluate the quality of performance of our four model structures. We start with the most basic evaluation, visual inspection of fit. Figure 4 presents the modeled data with the highest likelihood (in red) and the related uncertainty bandwidths (in green) together with the measured data (in blue) for each network. Visual inspection clearly shows that some networks perform better than others. The fit for the cumulative biogas is better in networks 2 – 4 and the fit for ammonium concentration is better in networks 3 – 4. In addition, the uncertainty is lower in networks 2 – 4 indicated by slightly narrower green bandwidths.

Visual judgment, however, reveals very little about the mechanistic correctness and parameter uncertainty in the models. The D_{KL} values in table 3 indicate the uncertainty of the calibrated parameters relative to the different model structures. Higher values mean lower uncertainty. The uncertainty in the calibration of $K_{inh, C_{VFA}}^{SL(meth)}$, for example, is much lower for network 2 – 4 than network 1. Preferably, we select a model with a low uncertainty in all calibrated parameters. The uncertainty in the total error for each subset of data is shown per network by the D_{KL} values of the standard deviations. This shows for instance that the uncertainty for the subset of ammonium is much lower in networks 3 – 4 than networks 1 – 2.

The posterior bandwidths (5%–95% quantiles) in table 3 reveal how close the calibrated parameters are to 'ideal' values measured under non-limiting conditions. Parameters that are close are indicated in bold. Ideally for mechanistic completeness, all calibrated parameters should be close to 'ideal' values. Network 2 – 4 are therefore more mechanistic correct than network 1 because the calibrated bandwidths of μ_{hyd}^{max} and μ_{meth}^{max} are closer to 'ideal' values.

Most parameters in the networks are not correlated except for the maximum rate and the half saturation constant of methanogenesis in the less complex networks. These correlations are presented in Figure 5. Interestingly, the correlation becomes weaker as the complexity and mechanistic information content of the model structures increases.

The log-normal marginal likelihoods-values in figure 4 show the performance of the networks with respect to the balance of information content (model complexity) versus model uncertainty. They show that although network 4 is most complex, the added information improves the maximum likelihood without increasing model uncertainty too much.

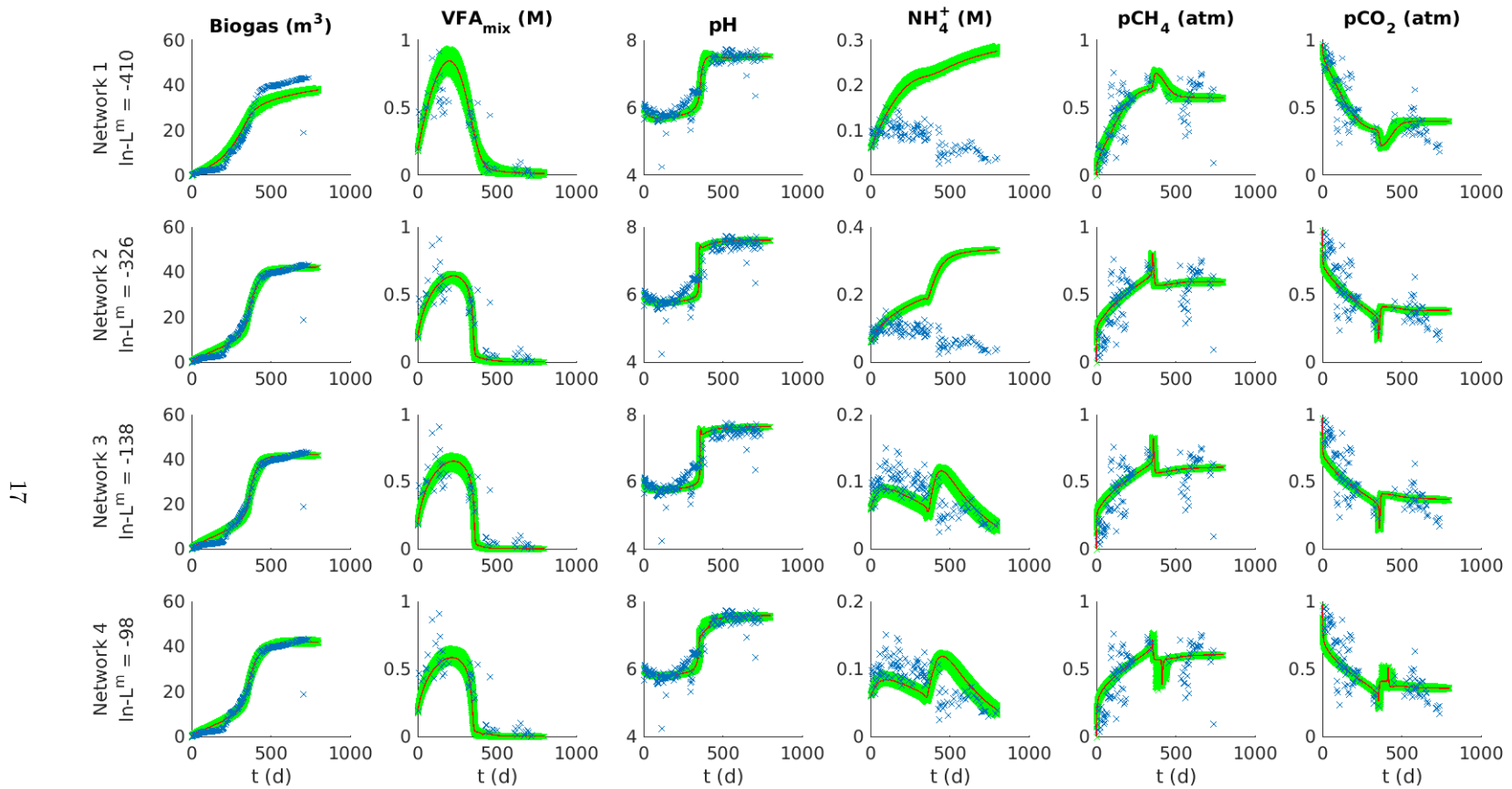
When evaluating model uncertainty based on statistics, it is important to check if the statistical assumptions applied are valid. This means that the probability of the residuals should be normally distributed because we apply a Gaussian likelihood. We check this with Q-Q plots and normalized autocorrelation functions (ACF) for the residuals of the best fit results of network 4 which are presented

1
2
3
4
5
6
7
8
9
10
11
12
13
14
15
16
17
18
19
20
21
22
23
24
25
26
27
28
29
30
31
32
33
34
35
36
37
38
39
40
41
42
43
44
45
46
47
48
49
50
51
52
53
54
55
56
57
58
59
60
61
62
63
64
65

in figure 6. The Q-Q plots show residual quantiles (in blue) vs quantiles from the theoretical normal distribution. When the residual quantiles are normally distributed they should coincide with the theoretical red line. Apparently, not all residuals are normally distributed. Therefore, some error is present in the statistical evidence we apply to evaluate our models. The same violation of normal distribution is indicated by the autocorrelation of the residuals. However, for the type of evaluations we apply this statistical error has minimal impact. If one is interested in a more statistical correct evaluation, we suggest to use the general likelihood function presented by Schoups and Vrugt et al. (2010)[33].

1
2
3
4
5
6
7
8
9
10
11
12
13
14
15
16
17
18
19
20
21
22
23
24
25
26
27
28
29
30
31
32
33
34
35
36
37
38
39
40
41
42
43
44
45
46
47
48
49

Figure 4: Measured data and best fit model results for the four reaction networks



\perp

Table 3: The prior ranges, posterior ranges (5% – 95% quantiles) and information gain (D_{KL}) for the inferred parameter per network

	$\mu_{\text{hyd}}^{\text{max}}$ (d^{-1})		$\mu_{\text{meth}}^{\text{max}}$ (d^{-1})		$K_{\text{inh}, C_{\text{VFA}}^{\text{T}}}^{\text{SL(meth)}}$ (mM)		$C_{\text{X}_{\text{meth}}}^{\text{T(ini)}}$ (mM)	
	quantiles	D_{KL}	quantiles	D_{KL}	quantiles	D_{KL}	quantiles	D_{KL}
Prior	0.09-0.26 [41]		0.04-0.47 [22]		0.03-420 [22]		0.27-19 [25]	
Network 1	0.004-0.0045	10.6	0.013-0.029	7.72	330-1318	2.12	8.6-13.5	5.70
Network 2	0.052-0.060	7.84	0.127-0.199	6.24	60-152	4.54	8.8-12.6	5.97
Network 3	0.056-0.069	7.30	0.095-0.167	6.23	95.5-184	4.54	12.9-25.3	4.83
Network 4	0.050-0.061	7.55	0.095-0.145	6.63	152-259	4.24	14.5-25.8	4.93

	$\mu_{\text{NH}_4}^{\text{max}}$ (d^{-1})		$\mu_{\text{sulph}}^{\text{max}}$ (d^{-1})		$K_{\text{inh}, C_{\text{SO}_4}^{\text{T}}}^{\text{SL(sulph)}}$ (mM)		$C_{\text{X}_{\text{sulph}}}^{\text{T(ini)}}$ (mM)	
	quantiles	D_{KL}	quantiles	D_{KL}	quantiles	D_{KL}	quantiles	D_{KL}
Prior	0.001-1		0.024-2.4 [31]		0.178-0.26 [30]		0.27-19 [25]	
Network 1								
Network 2								
Network 3	0.0044-0.0052	6.94						
Network 4	0.0043-0.0052	6.84	16.47-210	0.26	952-25085	1.06	0.095-120	2.95

	σ_{biogas} (m^3)		σ_{VFA} (mM)		σ_{pH}		$\sigma_{\text{NH}_4^+}$ (mM)	
	quantiles	D_{KL}	quantiles	D_{KL}	quantiles	D_{KL}	quantiles	D_{KL}
Prior	3.41-85.2		0.05-1.24		0.16-3.95		0.005-0.136	
Network 1	4.19-5.14	8.86	0.13-0.19	7.47	0.24-0.28	8.82	0.12-0.15	5.93
Network 2	2.12-2.52	9.76	0.12-0.17	7.62	0.27-0.32	8.86	0.14-0.17	5.76
Network 3	2.19-2.62	8.68	0.12-0.17	7.65	0.27-0.32	8.18	0.029-0.036	7.24
Network 4	2.06-2.49	9.64	0.12-0.17	7.58	0.23-0.26	9.11	0.029-0.038	7.06

	σ_{pCO_2} (atm)		σ_{pCH_4} (atm)	
	quantiles	D_{KL}	quantiles	D_{KL}
Prior	0.04-1.01		0.04-1.05	
Network 1	0.12-0.14	7.99	0.11-0.13	8.10
Network 2	0.13-0.16	7.89	0.13-0.16	7.91
Network 3	0.13-0.17	7.87	0.13-0.16	7.82
Network 4	0.13-0.17	7.82	0.13-0.16	7.79

Quantiles that are comparable with 'ideal' values measured under non-limiting conditions are presented in bold.

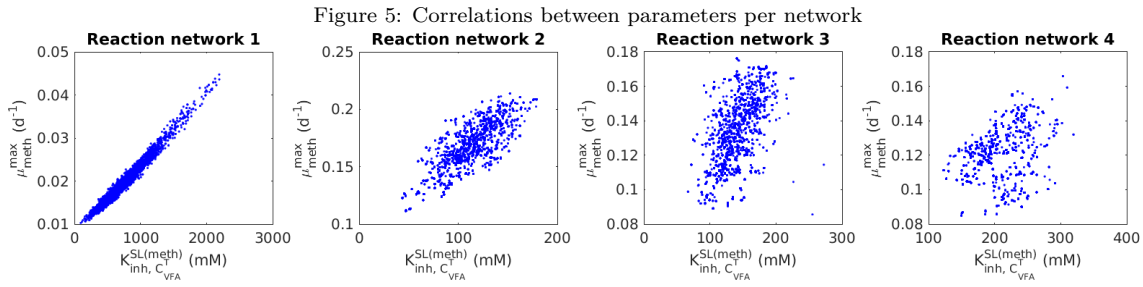
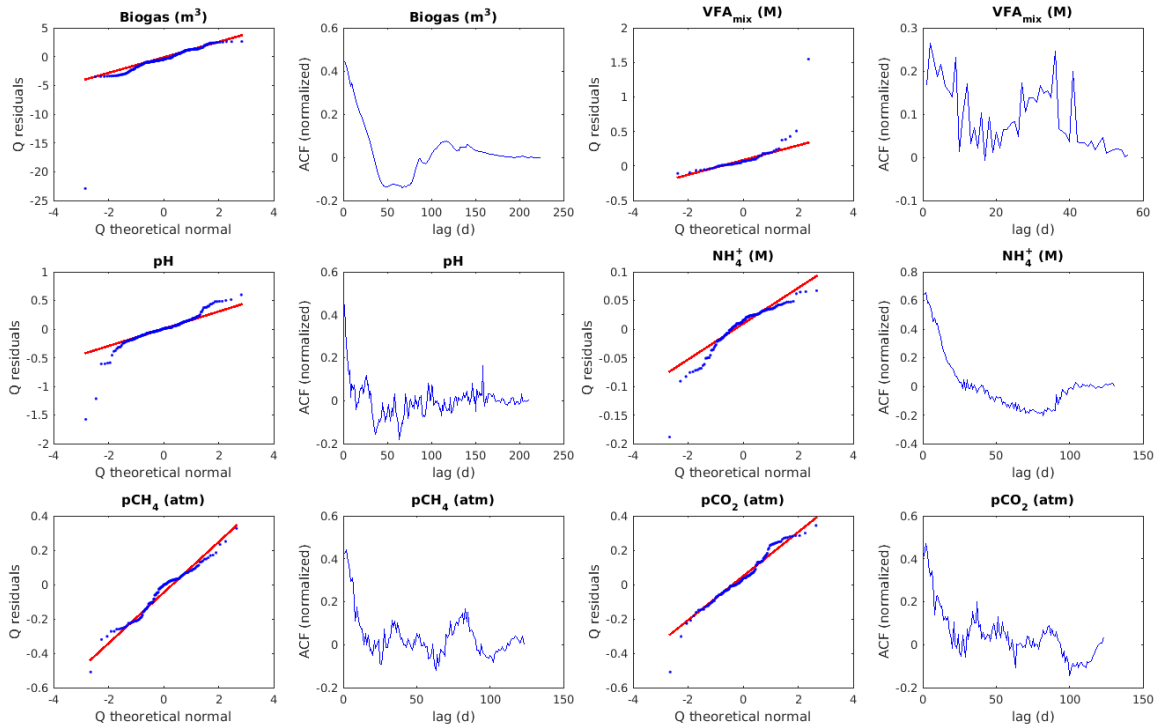


Figure 5: Correlations between parameters per network

Figure 6: Q-Q plots and autocorrelation functions (ACF) per sub dataset of the best fit residuals of reaction network 4



4. Discussion & Conclusions

The aim of the methods combined in the toolbox is to choose an optimal network with which we can describe anaerobic digestion of MSW. We believe this novel approach helps to reduce the ambiguity in model structure and calibrated parameter values reported in literature for a given environmental system. It strengthens (qualitative) judgment of model performance by providing quantitative criteria for evaluating (mechanistic) model uncertainty and it allows integrated environmental assessment. As a result, we obtain model structures which allow us to make predictions with a higher certainty because we have included more (objective) information for selecting the reaction network.

4.1. Performance of network 1

The most basic reaction network 1 reasonably reproduced a significant portion of the measured data (figure 4) with low uncertainty in total error (narrow green bandwidths). The model captures the values and trends of measured VFA_{mix} , pH, pCH_4 and pCO_2 in time. This good fit was achieved by selecting a set of reactions with the correct stoichiometry and parameter values from well established anaerobic reaction networks from literature, databases and derivation methods. The toolbox optimizes the implementation of such networks.

The model based on reaction network 1, however, does not provide a nice fit to all subsets of data. Using the results from the Bayesian inference, we modified the model structure in order to improve the results. Figure 5 shows that $K_{\text{inh}, C_{\text{VFA}}}^{\text{SL(meth)}}$ is strongly correlated with $\mu_{\text{meth}}^{\text{max}}$. This suggests that both parameters can be lumped together or that another process is being compensated for by the correlation of these two parameters. The results also show that the optimized values of probability distributions of the maximum rates are low compared to 'ideal' values. We concluded that limitations or inhibitions are missing in the reaction network which reduce prediction accuracy and cause the poor fit for cumulative biogas and ammonium.

4.2. Performance of network 2

Network 2 is extended with reaction terms which include the main environmental inhibitions acting on hydrolysis and methanogenesis. Assessing the results for this network indicate that this extension significantly improves the model fit of the cumulative biogas. In addition the calibrated maximum rates are in closer agreement with 'ideal' values. We conclude that the mechanistic description is more correct, while all parameters are still identifiable within sharp bandwidths (although some with slightly broader probability distributions than in network 1).

Adding the inhibition terms weakened the correlation between $K_{\text{inh}, C_{\text{VFA}}}^{\text{SL(meth)}}$ and $\mu_{\text{meth}}^{\text{max}}$. The value of $K_{\text{inh}, C_{\text{VFA}}}^{\text{SL(meth)}}$ is still high compared to 'ideal' values which indicates that this parameter compensates for a missing mass transport limitation in the model.

The difference in calibrated values between network 1 and network 2 nicely illustrates how easily ambiguity is created in published parameter values and outcomes of models [22]. By assuming a slightly different model structure, different sets of calibrated values will be reported which in turn may be used in yet again different model structures leading to wrong predictions. The only way to reduce this ambiguity is to report calibrated parameters together with the reaction networks and model structures from which they have been defined. Ideally the reactions should be mechanistically correct and the resulting parameters should be identifiable (i.e. possessing a narrow probability distribution without being correlated to other parameters). For this, statistical evaluation of model outcome and

1
2
3
4
5 parameter distributions is necessary because basic evaluation by eye does not give the information
6 needed to judge mechanistic correctness and identifiability.

7
8 In the case of reaction network 2, the evaluation indicates a structure that is nearly correct. How-
9
10
11
12
13
14
15
16
17
18
19
20
21
22
23
24
25
26
27
28
29
30
31
32
33
34
35
36
37
38
39
40
41
42
43
44
45
46
47
48
49
50
51
52
53
54
55
56
57
58
59
60
61
62
63
64
65

400 However, the concentration of ammonium is still overestimated by the model. This is to be expected since hydrolysis releases ammonium and the anaerobic reaction network 2 does not include an ammonium removal process. The experimental results clearly indicate that such a process occurs in the lysimeter.

4.3. Performance of network 3

In network 3, a relatively simple ammonium oxidation process is added to the reaction network. As a result, the model fit of the ammonium concentration improved drastically, while the rest of the model performance stayed similar to that of network 2. The modeled pH and the calibrated parameter bandwidths are not significantly influenced. The results indicate that in this lysimeter experiment an ammonium oxidation rate of 0.0048 d^{-1} is likely. The ammonium oxidation in the experiment was most likely caused by intrusion of oxygen when leachate was recirculated.

4.4. Performance of network 4

410 Although the results of network 3 are very good, we chose to do one more iteration. The waste used in the lysimeter most probably contained a source of sulphate (gypsum from building waste). This implies that sulphate reduction can occur which may explain the delay in onset of biogas production observed in the measured data. Although neither sulphate or sulphide were measured in this experiment, the results indicate an improved fit because both the errors in the fit of cumulative biogas and pH decreased. The final parameter distributions of the other parameters remained the same as found for network 3. The calibrated parameter values for sulphate reduction have a wide range and are high compared to 'ideal' values so we have to be careful in judging the mechanistic correctness of this approach. The improved datafit can be explained by the mechanism of sulphate reduction but it just as well can be attributed to the additional degrees of freedom added by the extra reaction. Measurements of sulphate and sulphide species are necessary to make a conclusion about how to improve the reaction network.

4.5. Selecting the optimal model structure for anaerobic digestion of MSW

4.5.1. For lysimeter scale

Based on the evaluation of network performances, we choose reaction network 3 as the optimal model structure for anaerobic digestion of MSW on a lysimeter scale. All parameters are either based on thermodynamic principles, taken from well established geochemical databases or calibrated with bandwidths which are in agreement with 'ideal' values. This strong mechanistic character of the

1
2
3
4
5 model together with its low uncertainty in calibrated parameters increases confidence in (long-term)
6 prediction accuracy compared to other model structures.

7
8
9 430 For the value of $K_{\text{inh},C_{\text{VFA}}^{\text{T}}}^{\text{SL(meth)}}$, we suggest to either keep it as a parameter to be calibrated as a 'material
10 property' for the system under investigation or to further extend the model with a transport limitation
11 mechanism such as diffusion with an extra transport parameter which then needs to be calibrated.
12

13 Network 4 is not preferred over network 3 because the mechanism of sulphate reduction can not
14 be adequately calibrated with this dataset. The improved likelihood is not guaranteed when applying
15 this reaction network to other experiments and conditions. Calibration of network 4 with an extended
16 435 measured dataset including sulphate or sulfide measurements would be very interesting.
17
18

19 Another interesting option would be to include the measurement error in the likelihood function.
20 This was not possible for this dataset since the measurement error was unknown. Nevertheless, when
21 included a distinction between model and measurement error could be made. A fully correct model
22 would by necessity include all measured data within the green uncertainty bandwidths in figure 4.
23 440
24

25 26 4.5.2. For full scale

27 For full scale application, we select network 2 as the optimal model structure. Network 2 is preferred
28 over network 3 because the ammonium oxidation in network 3 is modeled with a non-mechanistic
29 first order decay function based on the observations only. In this experiment, air intrusion during
30 recirculation of leachate is causing this degradation. This is probably not representative for large scale
31 445 anaerobic digestion of waste in landfills.
32
33
34
35
36

37 5. Acknowledgments

38
39 This research is supported by the Dutch Technology Foundation STW, which is part of the Nether-
40 lands Organization for Scientific Research (NWO), and which is partly funded by the Ministry of
41 Economic Affairs. We thank Roberto Valencia for providing us with the original data from his lysime-
42 450 ter experiments. We also thank Jasper Vrugt for providing us with a very efficient DREAM_{ZS} module
43 which is included in the toolbox. Furthermore, we like to thank Jasper Vrugt and the anonymous
44 reviewers for their comments which helped us to greatly improve the paper.
45
46
47
48
49

50 6. Supporting Information

51
52 455 The toolbox is implemented in MATLAB[19] and the algorithm is available at DOI: 10.4121/uuid:aefbaeb9-
53 85be-4fa6-a29e-a9cb71d0fb3a. Here, also a detailed manual is provided on how to use the toolbox. The
54 toolbox can be used without the requirement of special MATLAB toolboxes. Ordinary differential
55 equations are solved with ode15s. For the Bayesian inference, an efficient submodule of DREAM_{ZS} is
56
57
58

1
2
3
4
5 used and provided by Jasper Vrugt. A single integration of a network takes approximately 2.5 seconds
6
7 and a Bayesian inference run with 250.000 iterations takes approximately 1 week. Inference run time
8
9 can be substantially decreased ($\frac{1}{3}$) when Markov chains are run in parallel.

10
11 [1] Angelidaki, I., Ellegaard, L., Ahring, B.K., 1999. A comprehensive model of anaerobic biocon-
12 version of complex substrates to biogas. *Biotechnology and bioengineering* 63, 363-72. URL:
13 <http://www.ncbi.nlm.nih.gov/pubmed/10099616>.

14
15
16
17 [2] Atkins, P., de Paula, J., 2011. *Physical chemistry for the life sciences*. Freeman, W.H. URL:
18 http://books.google.nl/books/about/Physical_Chemistry_for_the_Life_Sciences.html?id=WPwA3EOXsOQC&

19
20 [3] Batstone, D.J., Keller, J., Angelidaki, I., Kalyuzhnyi, S.V., Pavlostathis, S.G., Rozzi, A., Sanders,
21 W.T.M., Siegrist, H., Vavilin, V.A., 2002. The IWA Anaerobic Digestion Model No 1 (ADM1).
22 *Water science and technology : a journal of the International Association on Water Pollution*
23 *Research* 45, 65-73. URL: <http://www.ncbi.nlm.nih.gov/pubmed/12188579>.

24
25
26
27 [4] Bennett, N.D., Croke, B.F.W., Guariso, G., Guillaume, J.H.A., Hamilton, S.H., Jakeman,
28 A.J., Marsili-Libelli, S., Newham, L.T.H., Norton, J.P., Perrin, C., Pierce, S.A., Robson,
29 B., Seppelt, R., Voinov, A.A., Fath, B.D., Andreassian, V., 2013. Characterising perfor-
30 mance of environmental models. *Environmental Modelling \& Software* 40, 1-20. URL:
31 <http://dx.doi.org/10.1016/j.envsoft.2012.09.011>, doi:10.1016/j.envsoft.2012.09.011.

32
33
34 [5] Bethke, C., 2008. *Geochemical and biogeochemical reaction mod-
35 eling*. Cambridge University Press, Cambridge U.K. URL:
36 http://www.langtoninfo.com/web_content/9780521875547_frontmatter.pdf.

37
38
39
40
41 [6] Fellner, J., Döberl, G., Allgaier, G., Brunner, P.H., 2009. Comparing field investiga-
42 tions with laboratory models to predict landfill leachate emissions. *Waste management*
43 (New York, N.Y.) 29, 1844-51. URL: <http://www.ncbi.nlm.nih.gov/pubmed/19171473>,
44 doi:10.1016/j.wasman.2008.12.022.

45
46
47
48 [7] Garcia de Cortazar, A.L., Monzon, I.T., 2007. MODUELO 2: A new version of an inte-
49 grated simulation model for municipal solid waste landfills. *Environmental Modelling \& Soft-
50 ware* 22, 59-72. URL: <http://linkinghub.elsevier.com/retrieve/pii/S1364815205002215>,
51 doi:10.1016/j.envsoft.2005.11.003.

52
53
54
55 [8] Gawande, N.A., Reinhart, D.R., Gour-Tsyh, Y., 2010. Modeling microbi-
56 ological and chemical processes in municipal solid waste bioreactor, Part II:
57
58

- 1
2
3
4
5 Application of numerical model BIOKEMOD-3P. Waste management (New
6 York, N.Y.) 30, 211–8. URL: <http://www.ncbi.nlm.nih.gov/pubmed/19815404>
490 <http://www.ncbi.nlm.nih.gov/pubmed/19819123>, doi:10.1016/j.wasman.2009.09.011.
8
9
- [9] Gönüllü, M., 1994. Analytical modelling of organic contaminants in leachate. Waste
10 management & research URL: <http://wmr.sagepub.com/content/12/2/141.short>
11 <http://wmr.sagepub.com/content/12/4/339.short>.
12
13
14
- 495 [10] Haldane, J., 1930. Enzymes. Journal of the Society of Chemical Industry 49, 919–920.
15
16
- [11] Heijnen, J.J., Kleerebezem, R., 1999. Bioenergetics of micro-
17 bial growth. Encyclopedia of Bioprocess Technology , 594–616URL:
18 <http://onlinelibrary.wiley.com/doi/10.1002/0471250589.ebt026/full>.
19
20
21
22
23
- [12] Henze, M., Harremoës, P., Jansen, J., Arvin, E., 1995. Wastewater Treatment - Biological and
24 Chemical Processes.
25
500
26
27
- [13] Kamalan, H., Sabour, M., Shariatmadari, N., 2011. A review on available land-
28 fill gas models. Journal of Environmental Science and Technology 4, 79–92. URL:
29 <http://agris.fao.org/agris-search/search/display.do?f=2012/DJ/DJ201229164103.xml;DJ2012029189>.
30
31
32
- [14] Karaca, F., Özkaya, B., 2006. NN-LEAP: A neural network-based model for controlling
33 leachate flow-rate in a municipal solid waste landfill site. Environmental Modelling & Software
34
505
35
36
37
38
39
- [15] Kelly, R.A., Jakeman, A.J., Barreteau, O., Borsuk, M.E., ElSawah, S., Hamilton, S.H.,
40 Henriksen, H.J., Kuikka, S., Maier, H.R., Rizzoli, A.E., van Delden, H., Voinov, A.A.,
41
42
43
510
44
45
46
47
48
49
2013. Selecting among five common modelling approaches for integrated environmental
assessment and management. Environmental Modelling & Software 47, 159–181. URL:
<http://www.scopus.com/inward/record.url?eid=2-s2.0-84879530766&partnerID=40&md5=adecc1fbe25545cf5>
doi:10.1016/j.envsoft.2013.05.005.
- [16] Kleerebezem, R., Van Loosdrecht, M.C.M., 2010. A Generalized Method for Thermodynamic
50
51
515
52
53
54
55
56
57
58
59
60
61
62
63
64
65

- 1
2
3
4
5
6 [17] Kouzeli-Katsiri, A., Bosdogianni, A., Christoulas, D., 1999. Prediction of leachate qual-
7 ity from sanitary landfills. *Journal of Environmental Engineering* 125, 950–958. URL:
8 [http://ascelibrary.org/doi/abs/10.1061/\(ASCE\)0733-9372\(1999\)125:10\(950\)](http://ascelibrary.org/doi/abs/10.1061/(ASCE)0733-9372(1999)125:10(950)).
9 520
- 10
11 [18] Laloy, E., Vrugt, J.A., 2012. High-dimensional posterior exploration of hydrologic mod-
12 els using multiple-try DREAM (ZS) and high-performance computing. *Water Resources Re-*
13 *search* 48, W01526. URL: <http://www.agu.org/pubs/crossref/2012/2011WR010608.shtml>,
14 doi:10.1029/2011WR010608.
15
16
17
18 525 [19] MATLAB Release 2015a, . The MathWorks, Inc.
- 19
20 [20] McDougall, J., 2007. A hydro-bio-mechanical model for settlement and other
21 behaviour in landfilled waste. *Computers and Geotechnics* 34, 297–320.
22 URL: <http://www.sciencedirect.com/science/article/pii/S0266352X07000158>
23 <http://linkinghub.elsevier.com/retrieve/pii/S0266352X07000158>,
24 doi:10.1016/j.compgeo.2007.02.004,
25 530
26
27
28 [21] Meeussen, J.C.L., 2003. ORCHESTRA: an object-oriented framework for implementing
29 chemical equilibrium models. *Environmental science & technology* 37, 1175–82. URL:
30 <http://www.ncbi.nlm.nih.gov/pubmed/12680672>.
31
32
33 [22] Meima, J.A., Naranjo, N.M., Haarstrick, A., 2008. Sensitivity analysis and literature review of pa-
34 rameters controlling local biodegradation processes in municipal solid waste landfills. *Waste man-*
35 *agement (New York, N.Y.)* 28, 904–18. URL: <http://www.ncbi.nlm.nih.gov/pubmed/17499984>,
36 535
37
38
39
40
41 [23] Monod, J., 1949. The growth of bacterial cultures. *Annual Reviews in Microbiology* URL:
42 <http://www.annualreviews.org/doi/pdf/10.1146/annurev.mi.03.100149.002103>.
43
44
45 540 [24] Newton, M.A., Raftery, A.E., 1994. Approximate Bayesian Inference with the Weighted
46 Likelihood Bootstrap. *Journal of the Royal Statistical Society* 56, 3–48. URL:
47 <http://www.jstor.org/stable/2346025>.
48
49
50 [25] Nopharatana, A., Pullammanappallil, P.C., Clarke, W.P., 2007. Kinetics and dynamic mod-
51 elling of batch anaerobic digestion of municipal solid waste in a stirred reactor. *Waste manage-*
52 *ment (New York, N.Y.)* 27, 595–603. URL: <http://www.ncbi.nlm.nih.gov/pubmed/16797956>,
53 545
54
55
56
57
58
59
60
61
62
63
64
65

- 1
2
3
4
5
6 [26] Ozkaya, B., Demir, A., Bilgili, M., 2007. Neural network prediction model for the methane
7 fraction in biogas from field-scale landfill bioreactors. *Environmental Modelling & Software*
8 22, 815–822. URL: <http://linkinghub.elsevier.com/retrieve/pii/S1364815206000776>,
9 doi:10.1016/j.envsoft.2006.03.004.
10 550
- 11
12 [27] Paula Jr, D.R., Foresti, E., 2009. Sulfide toxicity kinetics of a uasb re-
13 actor. *Brazilian Journal of Chemical Engineering* 26, 669–675. URL:
14 http://www.scielo.br/scielo.php?pid=S0104-66322009000400005&script=sci_arttext.
15
16
17
18 [28] Plummer, L.N., Busenburg, E., 1982. The solubilities of calcite, aragonite and vaterite in CO₂-
19 H₂O solutions between 0 and 90 C, and an evaluation of the aqueous model for the system
20 555 CaCO₃-CO₂-H₂O. *Geochimica et cosmochimica acta* 46.
21
22
23 [29] Reichel, T., Ivanova, L.K., Beaven, R.P., Haarstrick, A., 2007. Modeling Decomposi-
24 tion of MSW in a Consolidating Anaerobic Reactor. *Environmental Engineering Science*
25 24, 1072–1083. URL: <http://www.liebertonline.com/doi/abs/10.1089/ees.2006.0230>,
26
27
28 560 doi:10.1089/ees.2006.0230.
29
- 30 [30] Roychoudhury, A.N., Van Cappellen, P., Kostka, J.E., Viollier, E., 2003. Kinet-
31 ics of microbially mediated reactions: dissimilatory sulfate reduction in saltmarsh sed-
32 iments (Sapelo Island, Georgia, USA). *Estuarine, Coastal and Shelf Science* 56,
33 1001–1010. URL: <http://linkinghub.elsevier.com/retrieve/pii/S0272771402003256>,
34
35
36 565 doi:10.1016/S0272-7714(02)00325-6.
37
38
- 39 [31] Rzczycka, M., Blaszczyk, M., 2005. Growth and activity of sulphate-reducing bacteria in media
40 containing phosphogypsum and different sources of carbon. *Polish Journal of environmental*
41 *studies* 14, 891–895. URL: <http://6csnfn.pjoes.com/pdf/14.6/891-895.pdf>.
42
43
44 [32] Scharff, H., van Zomeren, A., van der Sloot, H.A., 2011. Landfill sustainability and
45 aftercare completion criteria. *Waste management & research : the journal of the In-*
46 570 *ternational Solid Wastes and Public Cleansing Association, ISWA* 29, 30–40. URL:
47 <http://www.ncbi.nlm.nih.gov/pubmed/20921059>, doi:10.1177/0734242X10384310.
48
49
50
51 [33] Schoups, G., Vrugt, J.A., 2010. A formal likelihood function for parameter and predictive in-
52 ference of hydrologic models with correlated, heteroscedastic, and non-Gaussian errors. *Wa-*
53 *ter Resources Research* 46, n/a–n/a. URL: <http://doi.wiley.com/10.1029/2009WR008933>,
54
55 575 doi:10.1029/2009WR008933.
56
57
58
59
60
61
62
63
64
65

- 1
2
3
4
5
6 [34] Siegrist, H., Vogt, D., Garcia-Heras, J.L., Gujer, W., 2002. Mathematical model for meso- and
7 thermophilic anaerobic sewage sludge digestion. *Environmental science & technology* 36, 1113–
8 23. URL: <http://www.ncbi.nlm.nih.gov/pubmed/11917999>.
9
- 10
11 580 [35] Valencia, R., den Hamer, D., Komboi, J., Lubberding, H.J., Gijzen, H.J., 2009a. Al-
12 ternative treatment for septic tank sludge: Co-digestion with municipal solid waste in
13 bioreactor landfill simulators. *Journal of Environmental Management* 90, 940–945. URL:
14 <http://dx.doi.org/10.1016/j.jenvman.2008.02.007>, doi:10.1016/j.jenvman.2008.02.007.
15
16
17
18 [36] Valencia, R., van der Zon, W., Woelders, H., Lubberding, H.J., Gijzen, H.J., 2009b. Achieving
19 "Final Storage Quality" of municipal solid waste in pilot scale bioreactor landfills. *Waste man-*
20 585 *agement (New York, N.Y.)* 29, 78–85. URL: <http://www.ncbi.nlm.nih.gov/pubmed/18406126>,
21 doi:10.1016/j.wasman.2008.02.008.
22
23
24
25 [37] Valencia, R., van der Zon, W., Woelders, H., Lubberding, H.J., Gijzen, H.J., 2009c. The ef-
26 fect of hydraulic conditions on waste stabilisation in bioreactor landfill simulators. *Bioresource*
27 *Technology* 100, 1754–1761. URL: <http://dx.doi.org/10.1016/j.biortech.2008.09.055>,
28 590 doi:10.1016/j.biortech.2008.09.055.
29
30
31
32 [38] Valencia, R., Zon, W.V.D., Woelders, H., Lubberding, H.J., Gijzen, H.J., 2011. Anam-
33 mox: an option for ammonium removal in bioreactor landfills. *Waste management*
34 *(New York, N.Y.)* 31, 2287–93. URL: <http://www.ncbi.nlm.nih.gov/pubmed/21795036>,
35 595 doi:10.1016/j.wasman.2011.06.012.
36
37
38
39 [39] Valencia Vazquez, R., 2008. ENHANCED STABILISATION OF MUNICIPAL SOLID WASTE IN
40 BIOREACTOR LANDFILLS. Ph.D. thesis. Wageningen University and UNESCO IHE Institute
41 for Water Education, Delft.
42
43
44 [40] Vavilin, V.A., Rytov, S.V., Lokshina, L.Y., Pavlostathis, S.G., Barlaz, M.A., 2003.
45 600 Distributed model of solid waste anaerobic digestion: effects of leachate recircula-
46 tion and pH adjustment. *Biotechnology and bioengineering* 81, 66–73. URL:
47 <http://www.ncbi.nlm.nih.gov/pubmed/12432582>, doi:10.1002/bit.10450.
48
49
50
51 [41] Veeken, A.H., Hamelers, B., 1999. Effect of temperature on hydrolysis rates
52 of selected biowaste components. *Bioresource technology* 69, 249–254. URL:
53 605 <http://www.sciencedirect.com/science/article/pii/S0960852498001886>.
54
55
56
57
58
59
60
61
62
63
64
65

- 1
2
3
4
5 [42] Veeken, A.H., Hamelers, B., 2000. Effect of substrate-seed mixing and leachate recir-
6 culation on solid state digestion of biowaste. *Water science and technology : a jour-*
7 *nal of the International Association on Water Pollution Research* 41, 255–62. URL:
8 <http://www.ncbi.nlm.nih.gov/pubmed/11382000>.
9
10
11
12 610 [43] Vrugt, J.A., 2016. Markov chain Monte Carlo simulation using the DREAM software pack-
13 age: Theory, concepts, and MATLAB implementation. *Environmental Modelling & Software* 75,
14 273–316. URL: <http://www.sciencedirect.com/science/article/pii/S1364815215300396>,
15 doi:10.1016/j.envsoft.2015.08.013.
16
17
18
19 [44] Vrugt, J.A., Gupta, H.V., Bouten, W., Sorooshian, S., 2003. A Shuf-
20 fled Complex Evolution Metropolis algorithm for optimization and uncer-
21 615 tainty assessment of hydrologic model parameters. *Water Resources Re-*
22 *search* 39. URL: <http://www.agu.org/pubs/crossref/2003/2002WR001642.shtml>,
23 doi:10.1029/2002WR001642.
24
25
26
27
28 [45] White, J., Robinson, J., Ren, Q., 2004. Modelling the biochemical degradation of
29 620 solid waste in landfills. *Waste management (New York, N.Y.)* 24, 227–40. URL:
30 <http://www.ncbi.nlm.nih.gov/pubmed/15016412>, doi:10.1016/j.wasman.2003.11.009.
31
32
33
34
35
36
37
38
39
40
41
42
43
44
45
46
47
48
49
50
51
52
53
54
55
56
57
58
59
60
61
62
63
64
65

Dear editor,

Thank you for your fast reply, we are very happy that our manuscript is considered for publication in Environmental Modelling & Software (EM&S). We also thank you for your additional comments which enabled us to improve the transparency and framing of the presented methodology and results. We double checked the grammar in the paper and changed the following according to your comments.

In line 55, we included two citations of papers from EM&S (Vrugt et al. (2016) and Kelly et al. (2013)) which express the need for a more objective integrated assessment of environmental systems. These are included to show that novel methods such as the one we present are necessary to decrease uncertainty in modeling of environmental systems. Our toolbox decreases model uncertainty by combining mechanistic information from different environmental fields and evaluating models based on qualitative and quantitative criteria.

In line 56, we included a reference to Bennett et al. (2013) who propose a generic evaluation procedure of model performance. Such an approach strengthens the credibility and relevance of modelling reported which is in line with the methodology we present. In lines 83-92, we indicate that our method supports all five evaluation steps proposed by Bennett et al. (2013). In our evaluation, however, the step of checking the data is minimal because the available measured data and information about its error was very limited. Nevertheless, we believe that the characteristics of our novel methodology are sufficiently demonstrated and that the best model is satisfactory given the scope of the paper.

In section 2.4, we added a subsection describing the qualitative performance criteria that are generated by the toolbox. In section 2.4.3, we justify our choice in quantitative criteria. We chose a set of criteria that enabled us to quantify aspects related to the (mechanistic) uncertainty of the models which is in line with the purpose of our modeling exercise. In addition, we indicate that other criteria suited for other modeling purposes are readily implemented.

Results and discussion are only slightly modified because we believe that the changes made in the introduction and theory already improved their framing and justification significantly. Furthermore, we modified the conclusion about the best model into two steps. First we conclude which model is best for lysimeter scale and then we conclude which model is best for full scale.

We thank you for your time and hope our paper is now fit to contribute to Environmental Modelling & Software.

Sincerely yours,

André van Turnhout

LaTeX Source Files

[Click here to download LaTeX Source Files: TEX_file.tar.gz](#)